

Densities of Si determined by an image digitizing technique in combination with an electrostatic levitator

K. Ohsaka, S. K. Chung and W.K. Rhim

Jet Propulsion Laboratory, California Institute of Technology

Pasadena, California 91109

and

J. C. Holzer

MEMC Electronic Materials inc.

St Peters, Missouri 63376

Abstract

We have determined the densities of Si in the liquid, $\rho_l(T)$, and solid, $\rho_s(T)$, states as a function of temperature, T , by employing an image digitizing technique and numerical calculation methods in combination with an electrostatic levitator. The obtained density data can be fit by the following equations

$$\rho_l(T) = \rho_l(T_m) - 1.71 \times 10^{-4}(T - T_m) - 1.61 \times 10^{-7}(T - T_m)^2 \quad (\text{g/cm}^3)$$

$$\rho_s(T) = \rho_s(T_m) - 2.63 \times 10^{-5}(T - T_m) \quad (\text{g/cm}^3)$$

where T_m is the melting point, 1687 K, and $\rho_l(T_m)$ and $\rho_s(T_m)$ are 2.580 and 2.311, respectively. The error involved in the determination is estimated to be ± 0.006 (g/cm³). The $\rho_l(T)$ value smoothly varies through T_m and does not indicate a reported anomalous density variation. The $\rho_l(T_m)$ value is 2 % larger than the literature value and the coefficient of the linear temperature dependence is approximately half of a reported value. The $\rho_s(T_m)$ value closely agrees with the literature value.

Density data is important in the investigation of the nature and behaviors of metals and alloys. For example, the density difference between a liquid and solid at the melting point is essential in understanding melting and solidification phenomena. For this reason, density measurements have been repeatedly performed over many years and the data has become more accurate in recent years because the existing techniques have improved or new techniques have been introduced. In the course of developing a novel material confinement technique, we have developed a system which allows measurement of the thermophysical properties of high temperature metals and alloys. The system consists of an electrostatic levitator and non-invasive diagnostic devices. The capability of the system includes the measurements of the density, specific heat, hemispherical total emissivity, surface tension and viscosity.² Advantages of the system are the elimination of contamination associated with the containers and rapid data acquisition. The system has been applied to measure the properties of several materials including a glass forming alloy³ and Si.²

Silicon is a basic material in the semiconductor industry and the crystal growth process has been continuously refined with the aid of numerical modeling to satisfy the never-ending demand for the perfect Si crystal. For modeling, the density of the liquid at melting point, $T_m = 1687$ K, is an essential parameter. A density value commonly referred to in the literature is 2.53 (g/cm^3)^{4,5} which was measured in the 1950s. Recently, Sasaki, Tokizaki, Terashima and Kimura reported a higher value, 2.556 (at 1725 K), which was measured by an improved Archimedian method.⁶ Waseda, Shinoda, Sugiyama, Takeda, Terashima and Toguri also provided an even higher value, 2.595 (at 1725 K), which was consistent with an X-ray diffraction analysis of the radial distribution function of the liquid.⁷ The new values are significantly higher than the literature value and they seem to be more accurate according to our preliminary measurement which yielded 2.56 at T_m .² Furthermore, Sasaki et al. showed an anomalous density variation whose origin was not identified. In order to clarify the above discrepancies and anomaly, we decided to

reinvestigate the densities of Si. After we completed the preliminary measurement and reported the result, we have refined the technique and have added a device to improve the accuracy of the measurement,

A spherical sample of typically 15 mg was levitated in a high vacuum environment ($\sim 10^{-6}$ torr) using the electrostatic force which counterbalanced gravity. Heating of the sample was provided by a high intensity xenon arc lamp. Cooling of the sample was achieved by natural radiative heat loss to the surroundings. The temperature of the sample was measured by a pyrometer. Also, the images of the levitated sample were stored on video tape. The density was determined from these images by employing an image digitizing technique and numerical calculation methods. The detailed description of the levitation system and the density measurement method are reported elsewhere.^{1,8} An additional device employed for the present measurement was a mechanical shutter placed in front of the xenon lamp. The device was necessary to momentarily block the high intensity light in order to obtain clear images of the sample at high temperatures.

Figure 1 shows a typical thermogram of a sample on cooling when the heating source is completely blocked. The temperature was measured by a three-color pyrometer whose emissivity was adjusted at T_{in} . As is seen, the sample is substantially undercooled (approximately -300 K) prior to the onset (indicated by the arrow) of crystallization. Due to recalescence, the sample temperature almost instantaneously rises to T_m (dot and dash line). Only one temperature is registered during recalescence, which indicates that the recalescence time is approximately 1/30 sec because the data acquisition rate of the pyrometer is 60 times per second. The subsequent temperature rise above T_m is due to an increase in the spectral emissivity upon solidification.

Figure 2 shows the density of a liquid sample, $\rho(T)$ as a function of temperature, T . The density is determined from the images taken during the cooling process whose thermogram is shown in Fig. 1. Unlike pure metals whose densities show a linear

temperature dependence, $\rho_l(T)$ shows a quadratic dependence which can be fit by the following equation:

$$\rho_l(T) = \rho_l(T_m) - 1.71 \times 10^{-4}(T - T_m) - 1.61 \times 10^{-7}(T - T_m)^2 \text{ (g/cm}^3\text{)} \quad (1)$$

where $\rho_l(T_m) = 2.580$. Eq. (1) is shown as the curve in the figure.

Figure 3 shows the densities of the solid and liquid, which were determined while a levitated sample went through the melting process. For this measurement, a nearly spherical solid sample was initially heated up near T_m . The sample was then gradually heated further by increasing the intensity of the xenon lamp until it was melted and superheated. The shutter was employed to obtain the clear images of the sample during the process. Approximate start and end of melting are indicated by the arrows. During melting, the sample temperature stayed at T_m . The density of the solid, $\rho_s(T_m) = 2.311$ (g/cm³) was determined by taking the average of the data near T_m . This value agrees with an often quoted value, 2.31, in the literature. The large scattering of the data is due to non-sphericity of the solid sample. During melting, the sample was slightly deformed because the two phases tended to separate owing to the density difference. This deformation caused the scattering of the data during melting. The density reaches the maximum at the end of melting. Once melting is completed, the temperature starts rising, which is seen as the decrease in the density. The density increase toward the end of the time is due to the temperature decrease after reaching the maximum.

Figure 4 shows the density of the solid, $\rho_s(T)$, as a function of temperature. For this measurement, a solid sample was heated up near T_m and then cooled by radiative heat loss to the surroundings. The temperature was measured by a single-color pyrometer which was capable of measuring the temperature down to 550 K. In Fig. 4, the density of the solid is combined with the densities in Figs. 2 and 3 for comparison. The large scattering of the data is mainly due to the non-sphericity of the sample. Since the sample was

randomly rotated, the accurate determination of the density was possible by collecting a large number of data and taking an average. The linear fit of the data is given by

$$\rho_s(T) = \rho_s(T_m) - 2.63 \times 10^{-5}(T - T_m) \text{ (g/cm}^3\text{)}. \quad (2)$$

The density at room temperature is calculated to be 2.347 (g/cm³). The coefficient of the temperature dependence agrees with the value measured with a more rigorous method.⁹

The error involved in the density determination is determined to be $\pm 0.2\%$, which excludes the errors in the sample temperature, and weight measurements. The liquid is rapidly evaporated during the experiment; therefore, the weight must be estimated from the weights determined before and after the experiment. This estimation introduces the error which could be as large as $\pm 3\%$. The error involved in the temperature measurement is expected to be minimal because the spectral emissivity of the liquid shows no temperature dependence.¹⁰ These additional errors may exist in the density shown in Fig. 2, but do not in the density shown in Fig. 3 because both the temperature and weight are precisely known for the density measurement at T_m . By taking into account above error analysis, the confidential range of the density of the liquid at T_m is determined to be 2.580 ± 0.006 (g/cm³). This value is higher than the literature value and close to the Sasaki and Waseda values. Another discrepancy from the literature value is the temperature dependence of the density. The reported linear dependence coefficient is -3.5×10^{-4} (g/cm³K).⁵ The present measurement shows the quadratic dependence and the coefficient of the linear term at T_m is approximately a half of the reported value.

Figure 5 shows the comparison of the present result with the Sasaki and Waseda results. Their density values were taken from the reports. The Sasaki and Waseda values are shown by the full circles and the open circles, respectively. The curve is the present result represented by Eq. (1). If we take into account the errors involved in the measurements, at above 1800 K, the present result and the Sasaki result agree each other,

including the temperature dependence. However, at below 1800 K, the Sasaki values show an anomalous variation especially near T_m . This anomaly was attributed to the transient effect of a sluggish structural transition.⁶ They showed that when a liquid was brought down to a lower temperature from a higher temperature, an initial density was small but it gradually increased over several hours and settled at a final density. The difference between the initial and final densities was as large as **0.005** (g/cm³). Since the cooling rate of the present measurement is much faster (~ 90 K/sec at T_m), the liquid in the present measurement has less time for the transition. Thus, the downward deviation of the Sasaki values may be explained by the transient effect since their measurement is performed after holding the sample at each temperature for 30 minutes.

A steep increase in the Sasaki values is seen near T_m ; however, this increase cannot be explained by the transient effect. The Sasaki values appear to become similar to the present values. A possible explanation of this anomaly is as follows: We accept their interpretation of the transient effect, i.e., the liquid goes through the structural transition to form a short range structure if it is held at temperatures below 1800 K. The structure of the liquid should resemble that of the solid, but either the diamond or graphite structure is qualified by considering the similarity between Si and C. The graphite structure may be more stable than the diamond structure at high temperatures. However, the diamond structure becomes more stable near T_m because it is the stable structure of the solid. If the diamond structure is denser than the graphite structure as it is true for solid C, the density of the liquid could show the steep increase near T_m as seen in the Sasaki result. When the liquid is rapidly cooled as in the present case, it may not have enough time to form the graphite structure but may still form the diamond structure near T_m because it is the necessary path for eventual solidification. The quadratic temperature dependence of $\rho(T)$ also indicates the structural transition. The density values at T_m measured on cooling (Fig. 2) and heating (Fig. 3) show no difference, which implies that the diamond structure also exists in the liquid upon heating. It is conceivable that the local diamond structure exists in the liquid which is in

equilibrium with the solid at T_m and the structure persistently exists even after the solid has disappeared upon the completion of melting.

This work represents one phase of research carried out at the Jet Propulsion Laboratory, California Institute of Technology, under contract with the National Aeronautics and Space Administration,

References

- 1 W. K. Rhim, S. K. Chung, D. Barber, K. F. Man, G. Gutt, A. J. Rulison and R. E. Spjut, *Rev. Sci. Instrum.* **64**, 2961 (1993).
- 2 W. K. Rhim, S. K. Chung, A. J. Rulison and R. E. Spjut, *Int. J. Thermophys.* Accepted for publication
- 3 Y. J. Kim, R. Busch, W. L. Johnson, A. J. Rulison and W. K. Rhim, *Appl. Phys. Lett.* **68**, 1057 (1996).
- 4 V. M. Glazov, S. N. Chizhevskaya and N. N. Glagoleva, *Liquid Semiconductors* (Plenum Press, New York 1969).
- 5 T. Lids and R. I. L. Guthrie, *The Physical Properties of Liquid Metals* (Oxford University Press, 1988).
- 6 H. Sasaki, E. Tokizaki, K. Terashima and S. Kimura, (a) *Jpn. J. Appl. Phys.* **33**, 3803 (1994), (b) *J. Cryst. Growth* **139**, 225 (1994), (c) *Jpn. J. Appl. Phys.* **33**, 6078 (1994).
- 7 Y. Waseda, K. Shinoda, K. Sugiyama, S. Takeda, K. Terashima and J. M. Toguri, *Jpn. J. Appl. Phys.* **34**, 4124 (1995).
- 8 S. K. Chung, D. B. Thiessen and W. K. Rhim, *Rev. Sci. Instrum.* accepted for publication.
- 9 M. Okaji, *Int. J. Thermophys.* **9**, 1101 (1988).
- 10 S. Krishnan, J. K. R. Weber, P. C. Nordine, R. A. Schiffman, R. H. Hauge and J. L. Margrave, *High Temp. Science* **30**, 137 (1991).

Captions

Figure 1. A typical thermogram of a sample upon cooling. The maximum undercooling level is approximately 300 K prior to the onset of crystallization indicated by the arrow.

Figure 2. The density of the liquid as a function of temperature. The curve is given by Eq. (1). The density at T_m is determined to be 2.580 (g/cm³).

Figure 3. The densities of the solid and liquid at T_m , which are determined while the sample goes through melting process. The approximate start and end of melting are indicated by the arrows.

Figure 4. The density of the solid as a function of temperature, The data in Figs. 1 and 2 are also shown for easy comparison.

Figure 5. The comparison of the present result with the Sasaki (full circles) and Waseda (open circles) results. The present result is represented by Eq. (1).

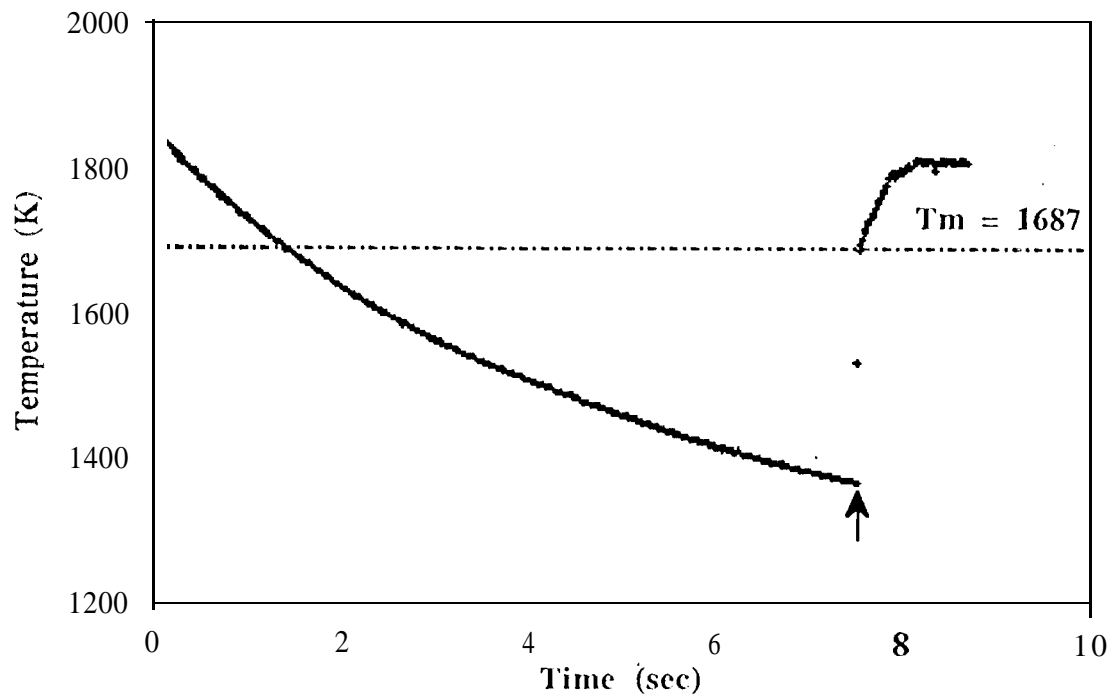
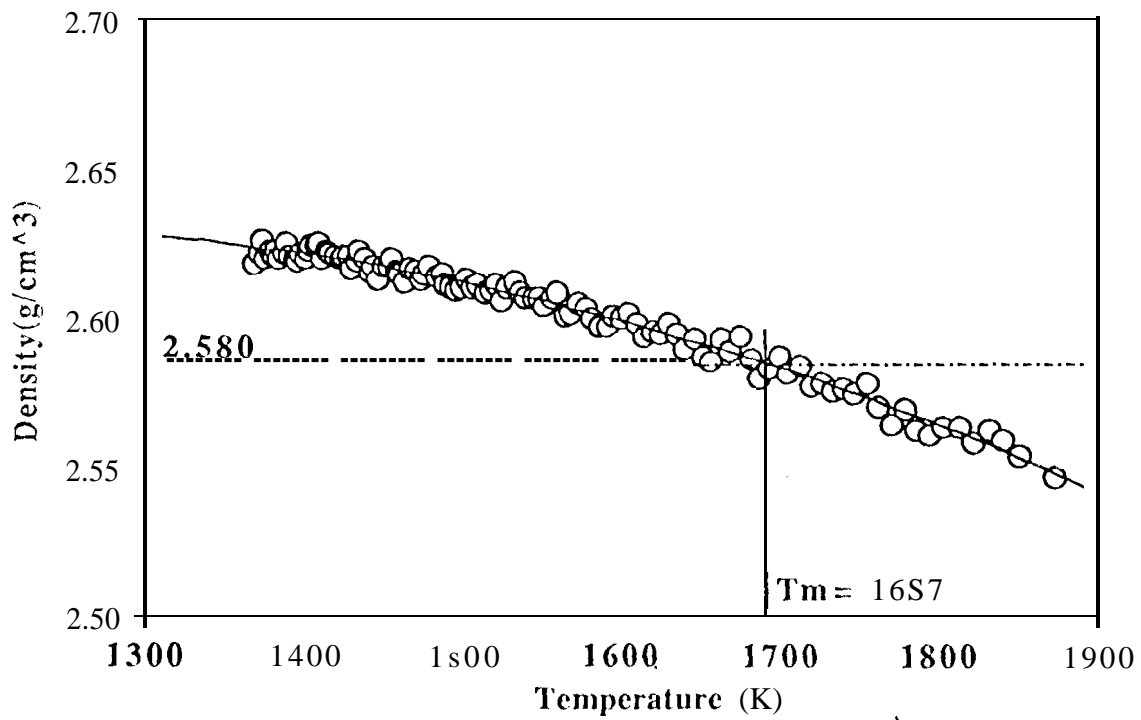


Fig. 1



\bar{r}_2

877-

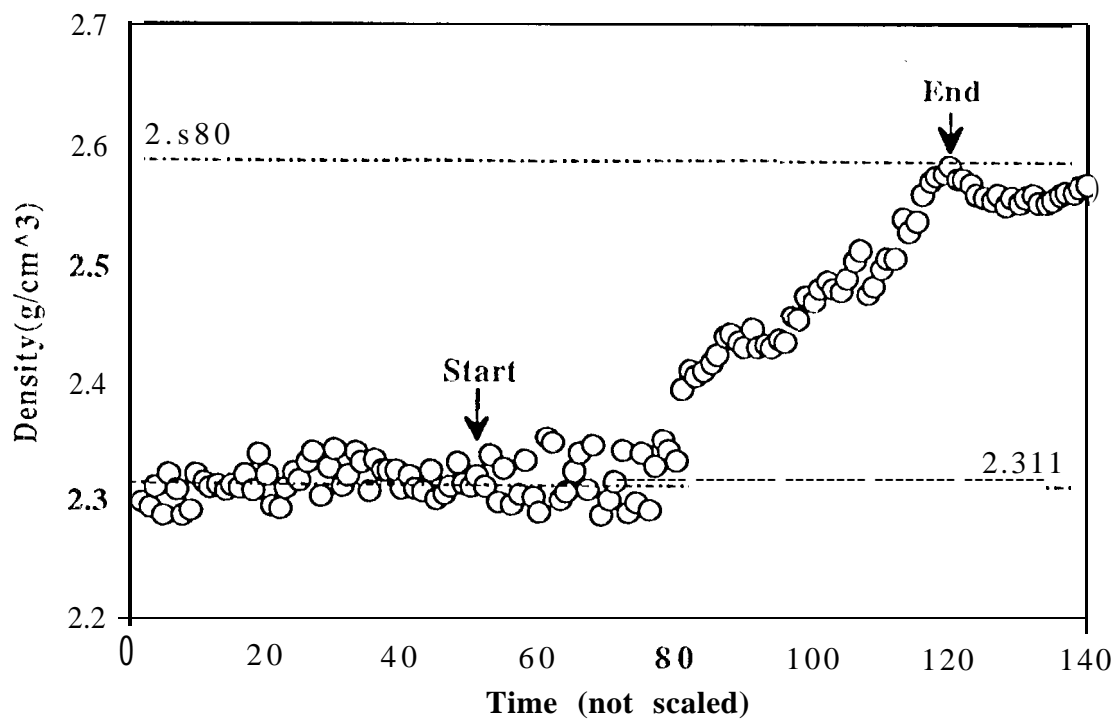


Fig. 3

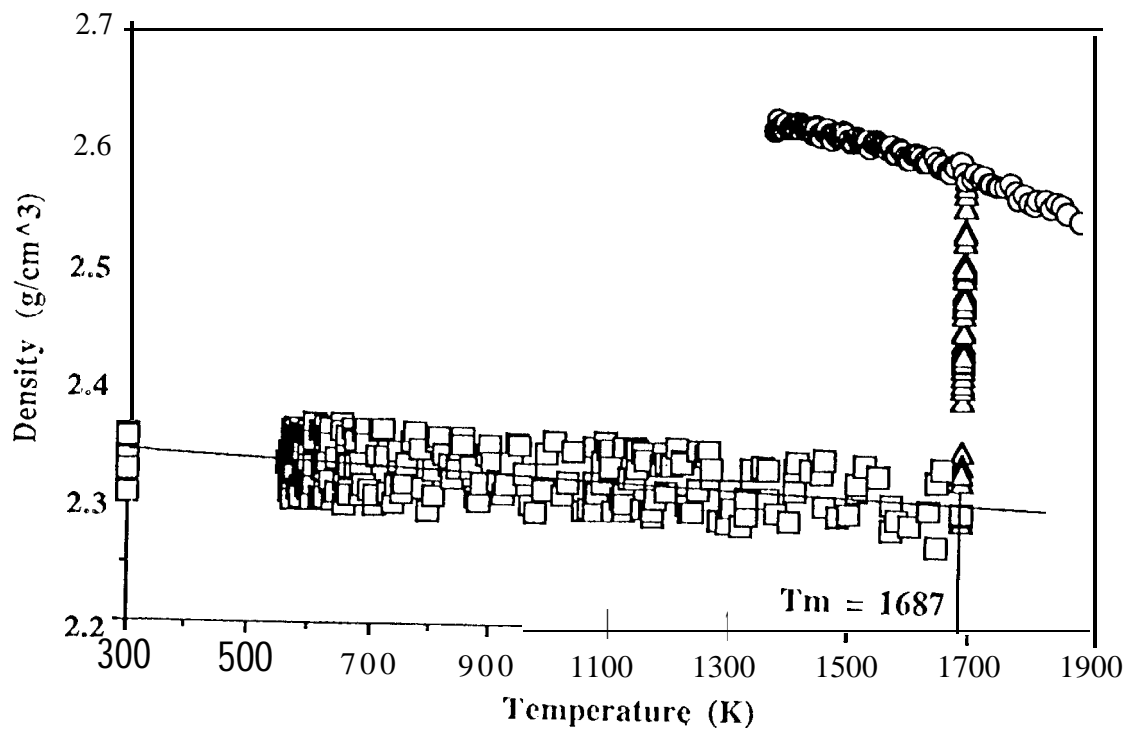


Fig. 4

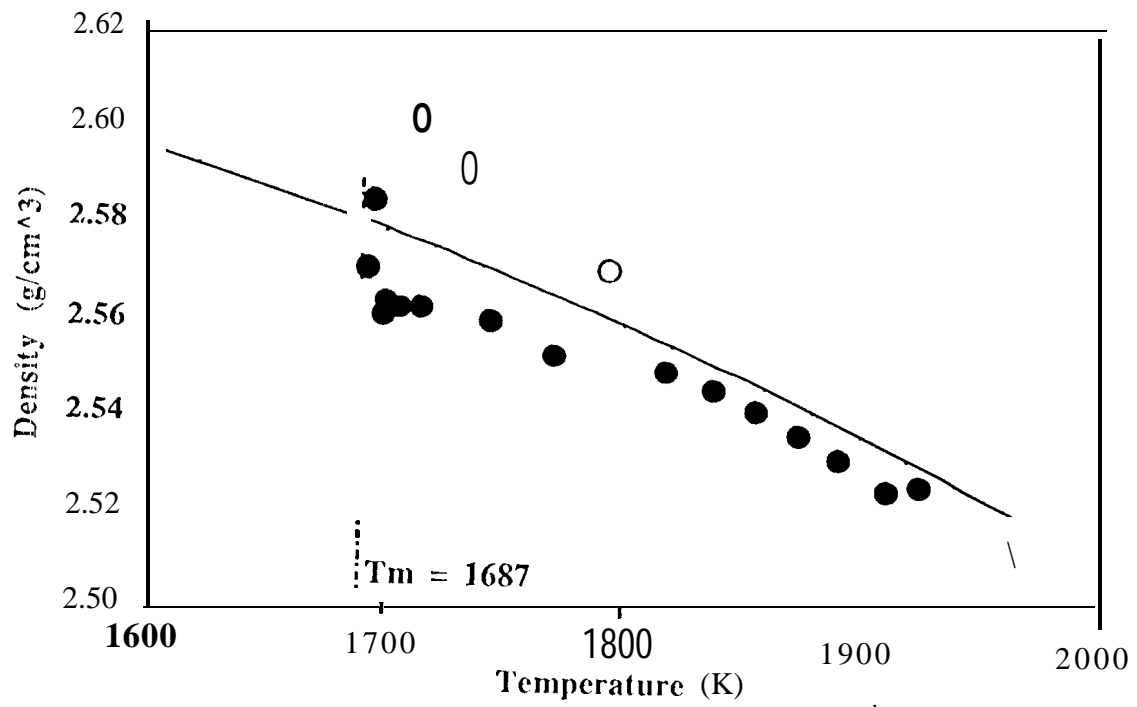


Fig. 5